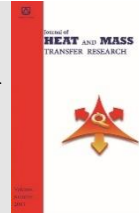




Semnan University



Estimation of Parameters and Selection of Models Applied to Population Balance Dynamics Via Approximate Bayesian Computational

Carlos Henrique Rodrigues de Moura^{a,ib}, Bruno Marques Viegas^{d,ib}, Maria Regina Madruga Tavares^{b,ib}, Emanuel Negrão Macêdo^{a,c,ib}, Diego Cardoso Estumano^{*,d,ib}

^a Graduate Program in Chemical Engineering, PPGEQ/ITEC/UFPA, Federal University of Pará, Belém, PA, Brazil

^b Graduate Program in Mathematics and Statistics, Federal University of Para, Belém, PA, Brazil.

^c Natural Resources Engineering, Federal University of Para, Belém, PA, Brazil.

^d School of Biotechnology and Bioprocess Engineering, Federal University of Para, Belém, PA, Brazil.

PAPER INFO

Paper history:

Received: 2021-11-09

Revised: 2022-06-19

Accepted: 2022-06-19

Keywords:

Particulate systems;
Population balance;
Bayesian statistics;
Approximate;
Bayesian computation;

ABSTRACT

Population balance models mathematically describe the particle size distribution based on modeling physical phenomena that influence the distribution, such as aggregation, growth, and breakage. Due to the wide range of mechanisms present, several models are presented in the literature since several hypotheses are considered. In the current work, the Approximate Bayesian Computational statistical technique was used to select four different models of population balance and estimate their parameters. Three strategies were applied to the drawing of parameters, evaluating the correlation between the parameters of the models. An adaptive tolerance in each population and a stopping criterion, based on Morozov's uncertainty principle, were used for the algorithm. The technique obtained reasonable estimates for the phenomenological rates of the models. The algorithm correctly selected the model used for generating measurements, and the three draw strategies demonstrated good applicability. The results obtained showed that the algorithm presented accuracy and precision in estimating the parameters and properly selected the models analyzed.

DOI: [10.22075/jhmtr.2022.25186.1361](https://doi.org/10.22075/jhmtr.2022.25186.1361)

© 2022 Published by Semnan University Press. All rights reserved.

1. Introduction

Particulate processes are present in several areas: agriculture [1], chemical engineering [2,3], pharmacy [4], and biotechnology [5,6]. A characteristic property of these processes is the particle size distribution, which is time-dependent about its average size and shape [7-9]. The particle size distribution is defined according to the mechanisms that govern the dynamics of particles in the medium, such as nucleation, growth, aggregation, and breakage.

In general, the mathematical models of this phenomenon are represented by partial and nonlinear integral-differential equations, called population balance equations [10-15]. The modeling of these equations is an area of application in expansion, especially in crystallization and precipitation [16],

polymerization [17], aerosol [18], and applications in biological systems [19].

Since several mechanisms cause this physical-chemical phenomenon, different models can be proposed according to the adopted hypotheses. The difficulty, however, lies in selecting the models that best describe the phenomenon to be studied. In addition, each model has its respective parameters. Therefore, applying statistical techniques capable of selecting models and estimating parameters is a practical approach in this area [20-24].

In this research, the Approximate Bayesian Computational (ABC) technique was used to simultaneously select models and estimate parameters. This selection will be possible to determine which physical phenomenon is

*Corresponding Author: Diego Cardoso Estumano
Email: dcestumano@ufpa.br

predominant from the analyzed data. In addition, models that describe the dynamics of a chemically homogeneous particulate system and its spatial state will be evaluated.

2. Mathematical model

Several phenomena influence the particle size distribution, mainly nucleation, growth, aggregation, and breaking [10]. An illustration of this phenomenon is shown in Figure. 1.

Population balance equations are models responsible for simulating the dynamics of these systems, Figure 1, which can be represented mathematically by Eq. (1) [25-28]:

$$\frac{\partial n(v, t)}{\partial t} = - \frac{\partial [I_v(v, t)n(v, t)]}{\partial v} + \frac{1}{2} \int_0^v \beta_v(v - \bar{v}, \bar{v}, t)n(v - \bar{v}, t)n(\bar{v}, t)d\bar{v} - \int_0^\infty \beta_v(v, \bar{v}, t)n(v, t)n(\bar{v}, t)d\bar{v} + S_v[n(v, t), v, t] \quad (1)$$

where $I_v(v, t)$ is the rate of change in volume v by mass transfer between particles and fluid phase; $\beta_v(v, \bar{v})$ is the coagulation coefficient of the particle for volumes v and \bar{v} ; and S_v is the net rate of addition or removal of particles in the system.

In Eq. (1), the term (I) is related to the rate of growth of particles by mass transfer to a single particle; the parcel (II) represents the generation of particles by the collision of particles with different sizes (assuming the conservation of volume during coagulation); the quantity (III) represents the rate of particle death from the collision with other particles; the term (IV) represents the rate of addition or removal of particles in the system.

Eq. (1) can be applied in colloidal chemistry, aerosol dynamics, crystallization kinetics, and biological population dynamics. Gelbard and Seinfeld [27] proposed four models, which are particular cases of Eq. (1), detailed in the following topics. However, it is essential to note that these models do not represent a single way of simulating the dynamics of particulate processes with others in the literature [29-33].

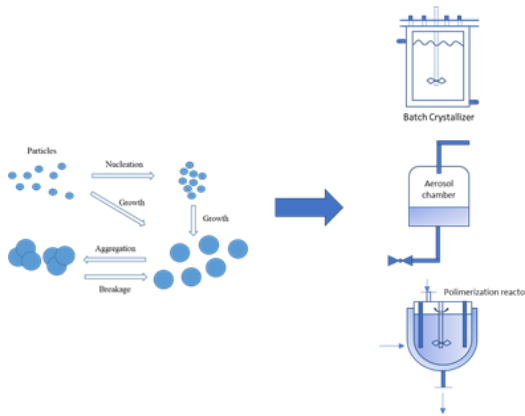


Figure 1. Phenomena that govern the distribution of particles. Adapted from [61]

2.1. Pure aggregation model with constant aggregation coefficient - Model 1

Model 1 considers a particulate system in which only pure aggregation is the phenomenon of interest and constant aggregation coefficient, $\beta_v(v, \bar{v}, t) = \beta_0(t)$. In this model, the step of random coalescence controls the process of enlarging the particles. Therefore, it means that the particles' size is not considered when forming a stable agglomerate and that the coefficient is independent of the size [34]. Thus, the population balance model in Eq. (1) takes the following form [26-28, 35]:

$$\frac{\partial n(v, t)}{\partial t} = \frac{\beta_0}{2} \int_0^v n(v - \bar{v}, t)n(\bar{v}, t)d\bar{v} - \beta_0 \int_0^\infty n(v, t)n(\bar{v}, t)d\bar{v} \quad (2)$$

where $\beta_0(t)$ is the constant aggregation coefficient, Applying the Laplace transform, Eq. (2) is reduced to Eq. (3) [35].

$$n(v, t) = \frac{4 \left(\frac{N_0}{v_0} \right)}{(2 + \beta_0 N_0 t)^2} \exp \left[- \frac{2}{(2 + \beta_0 N_0 t)} \frac{v}{v_0} \right] \quad (3)$$

In terms of the particle diameter, Eq. (3) becomes:

$$n(D, t) = \frac{4 \left(\frac{N_0}{v_0} \right) \left(\frac{D}{D_0} \right)^2}{(2 + \beta_0 N_0 t)^2} \exp \left[- \frac{2}{(2 + \beta_0 N_0 t)} \left(\frac{D}{D_0} \right)^3 \right] \quad (4)$$

2.2. Pure aggregation model with linear aggregation coefficient - Model 2

Model 2 considers that in the aggregation process, the colliding particle size contributes to forming an agglomerate, where larger particles have a more favorable agglomeration than the smaller ones [36]. The agglomeration coefficient takes the form $\beta_v(v, \bar{v}, t) = \beta_1(v + \bar{v})$, which is related to the turbulent diffusion in the medium [37, 38]. Thus, Eq. (1) takes the following form [26, 28, 35-37]:

$$\frac{\partial n(v, t)}{\partial t} = \frac{\beta_1}{2} \int_0^v (v + \bar{v})n(v - \bar{v}, t)n(\bar{v}, t)d\bar{v} - \beta_1 n(v, t) \int_0^\infty (v + \bar{v})n(\bar{v}, t)d\bar{v} \quad (5)$$

where β_1 is the linear aggregation coefficient. The mathematical model obtained by the partial integral-differential expression, Eq. (5), admits an analytical solution [35, 37].

$$n(v, t) = \frac{N_0(1 - T)}{v\sqrt{T}} \exp \left[- \frac{(1 + T)v}{v_0} \right] I_1 \left[2\sqrt{T} \frac{v}{v_0} \right] \quad (6)$$

where $T = 1 - \exp(-\tau)$, $\tau = \beta_1 N_0 v_0 t$, and I_1 is the modified first order Bessel function. In terms of the particle diameter, Equation (6) becomes:

$$n(D, t) = -\frac{3N_0(1-T)}{D\sqrt{T}} \exp\left[-\frac{(1+T)D}{D_0^3}\right] I_1\left[2\sqrt{T}\left(\frac{D}{D_0}\right)^3\right] \quad (7)$$

2.3. Pure aggregation model with linear aggregation coefficient and particle removal rate - Model 3

Model 3 considers a particulate system submitted to pure aggregation, whose linear agglomeration coefficient is equal to $\beta_1(v + \bar{v})$ and R_0 is the particle removal rate. The loss of particles to the container's inner surfaces can also be an important factor in changing the forms of particle size distribution. The main mechanisms for removing particles due to deposition are sedimentation and diffusion [39]. The population balance model for this case is presented as [27, 28]:

$$\frac{\partial n(v, t)}{\partial t} = \frac{\beta_1}{2} \int_0^v (v + \bar{v}) n(v - \bar{v}, t) n(\bar{v}, t) d\bar{v} - \beta_1 n(v, t) \int_0^\infty (v + \bar{v}) n(\bar{v}, t) d\bar{v} - R_0 n(v, t) \quad (8)$$

where β_1 is the linear aggregation coefficient and R_0 is the particle removal rate, Eq. (8) admits an analytical solution in the form [27,28]:

$$n(v, t) = -\frac{\tilde{T}N_0}{v\sqrt{\tilde{g}}} \exp\left[\frac{\tilde{T}-1}{\Theta}\right] \exp\left[-(1+\tilde{g})\frac{v}{v_0}\right] I_1\left[2\sqrt{\tilde{g}}\frac{v}{v_0}\right] \quad (9)$$

where $\tilde{T} = \exp(-\Theta\tau)$, $\tau = \beta_1 N_0 v_0 t$, $\tilde{g} = 1 - \exp(\tilde{T} - 1/\Theta)$, $\Theta = R_0/\beta_1 N_0 v_0$ and I_1 is the modified first order Bessel function. In terms of the particle diameter:

$$n(D, t) = -\frac{3\tilde{T}N_0}{D\sqrt{\tilde{g}}} \exp\left[\frac{\tilde{T}-1}{\Theta}\right] \exp\left[-(1+\tilde{g})\left(\frac{D}{D_0}\right)^3\right] I_1\left[2\sqrt{\tilde{g}}\left(\frac{D}{D_0}\right)^3\right] \quad (10)$$

2.4. Pure aggregation model with constant aggregation coefficient and linear growth rate - Model 4

Model 4 considers a particulate system submitted to pure aggregation, whose agglomeration coefficient is constant and the particle growth rate by condensation is heterogeneous. Thus, the growth term in Eq. (1) takes the form $I_v(v, t) = \sigma v$. Therefore, the population balance model is represented mathematically as [27, 28, 38]:

$$\frac{\partial n(v, t)}{\partial t} = -\sigma \frac{\partial [vn(v, t)]}{\partial v} + \frac{\beta_0}{2} \int_0^v n(v - \bar{v}, t) n(\bar{v}, t) d\bar{v} - \beta_0 \int_0^\infty n(v, t) n(\bar{v}, t) d\bar{v} \quad (11)$$

where σ represents the difference in the concentration of diffusing species in the environment and on the particle surface, considering a growth rate controlled by the medium's chemical reaction. The analytical solution for Eq. (11) is given by [27, 28]:

$$n(v, t) = \frac{4\left(N_0/v_0\right)}{(2+\tau)^2} \exp\left[-\frac{2v}{(2+\tau)v_0} \exp[-\Lambda\tau] - \Lambda\tau\right] \quad (12)$$

where $\Lambda = \sigma/\beta_0 N_0$. In terms of the particle diameter:

$$n(D, t) = \frac{4\left(N_0/v_0\right)\left(D/D_0\right)^2}{(2+\tau)^2} \exp\left[-\frac{2D^3}{(2+\tau)D_0^3} \exp[-\Lambda\tau] - \Lambda\tau\right] \quad (13)$$

3. Inverse problem

Prediction of measurements requires a mathematical model of the system under investigation. This prediction of observations, based on the values of the parameters that define the model, constitutes a straightforward problem. On the other hand, the inverse problem consists of using the observations' results to infer the values of the parameters and state variables that do not have measures for the system under investigation [40]. Bayes' theorem is the mechanism that combines the information obtained by the experiments with that of the mathematical model. Considering a vector of parameters, $\theta^T = [\theta_1, \theta_2, \theta_3, \dots, \theta_p]$, and a vector of measurements, $Y^T = [Y_1, Y_2, Y_3, \dots, Y_m]$, p and m represent the number of parameters and measures, respectively. Thus, Bayes' theorem can be defined as [41-46]:

$$\pi(\theta|Y^{meas}) \propto \pi_{prior}(\theta)\pi(Y^{meas}|\theta) \quad (14)$$

where $\pi(\theta|Y^{meas})$ represents the probability density *a posteriori*; $\pi_{prior}(\theta)$ is the prior probability density of the parameters; $\pi(Y^{meas}|\theta)$ it is the likelihood function. It can be observed by Bayes' theorem, Equation (14), that the solution of the inverse problem within the Bayesian approach seeks to obtain a probability distribution for the parameters, not being reduced to a set of point values of parameters, as in the techniques of traditional inference. In the form of a posteriori probability density, this distribution gathers prior knowledge about parameters, the mathematical model, and experimental data as information [41-46].

3.1. Approximate Bayesian Computation

In some cases, the likelihood is computationally intractable, and thus, it is difficult to estimate the *a posteriori* probability distribution of the parameters. Alternatively, one can use the Approximate Bayesian Computational technique, which replaces the likelihood calculation with statistical metrics related to the observed and simulated data [47]. This technique can be used simultaneously for model selection and for estimating parameters [48-50].

Given a prior probability distribution, the goal is to obtain an *a posteriori* probability distribution, $\pi(\theta|Y^{meas}) \propto \pi_{prior}(\theta)\pi(Y^{meas}|\theta)$, for the parameter vector to be estimated, where $\pi(Y^{meas}|\theta)$ is the likelihood function provided by the observed data Y^{meas} . However, a data set Y^* can be simulated from a value $\theta = \theta^*$. θ^* will be considered a posteriori sample if the pre-defined distance $d(Y^{meas}, Y^*)$ between the simulated and observed data is less than a limit value, defined as tolerance ε . For low values of ε , the distribution $\pi(\theta|d(Y^{meas}, Y^*) \leq \varepsilon)$ will adequately describe the *a posteriori* probability distribution $\pi(\theta|Y^{meas})$ [47-55].

The ABC algorithms are based on the following algorithm [48-53]:

1. Sample a vector of parameters θ^* from the prior probability distribution $\pi(\theta)$: $\theta^* \sim \pi(\theta)$;
2. Simulate a model data set $Y^* \equiv f(\theta^*)$, such that f is the straightforward model solution;
3. Compare the simulated data set Y^* , with experimental data, Y^{meas} , using a distance function, d , and a tolerance ε ; accept θ^* if $(Y^{meas}, Y^*) \leq \varepsilon$. Tolerance $\varepsilon \geq 0$ is the desired level of agreement between Y^{meas} and Y^* .

The term $d(Y^{meas}, Y^*)$ represents the Euclidean distance between the simulated and experimental data, and ε is the tolerance. The ABC algorithm generates a sample of parameters from a distribution $\pi(\theta|d(Y^{meas}, Y^*) \leq \varepsilon)$. This distribution will be a good approximation for the posterior distribution $\pi(\theta|Y^{meas})$ if ε is small enough [50].

In addition to its importance in estimating parameters within a Bayesian approach, the ABC algorithm can also select models. The model selection problem is addressed within the framework by including an additional discrete parameter $m \in \{1, \dots, M\}$, where M is the number of models. Model-specific parameters are represented by the function $\theta(m) = \{\theta_m^{(1)}, \dots, \theta_m^{(k_m)}\}$, where k_m indicates the number of model parameters m . Each population is started by sampling a model indicator m from the distribution of the last population, $\pi_{pop-1}(m)$. For the model m , new particles are proposed from a variation applied to the particles of the previous population (specific to m); this step is the same as in the parameter estimation algorithm. Particle weights $w(m)$ are also calculated in a similarly to the parameter estimation

algorithm for m . The ABC SMC algorithm for model selection proceeds as follows [48, 56, 57]:

1. Initialize $\varepsilon_1, \dots, \varepsilon_N$, where N_{pop} is the number of populations;
2. Set the population indicator $pop = 1$;
3. Set the particle indicator $i=1$;
4. Sample the model m^* from $\pi(m)$.
5. If $pop = 1$, draws θ^{**} from model m^* , $\theta^{**} \sim \pi(\theta|m^*)$. If $pop > 1$, draws θ^* from the previous population $\{\theta(m^*)_{pop-1}\}$ with weights $w(m^*)_{pop-1}$ and perturbrates the particle θ^* to obtain $\theta^{**} \sim K_{pop}(\theta|\theta^*)$. If $\pi(\theta^{**}) = 0$, returns to 3;
6. Simulate a candidate data set $Y^* \sim \pi(Y|\theta^{**}, m)$. If $d(Y^{meas}|Y^*) \geq \varepsilon_{pop}$, returns to 3;
7. Set $m_{pop}^{(i)} = m^*$, adds θ^{**} for the particle population $\{\theta(m^*)_{pop-1}\}$ and calculate the particle weight θ^{**} ,

$$w_{pop}^{(i)} = \begin{cases} 1 & , \text{if } pop = 1 \\ \frac{\pi(\theta^{**})}{\sum_{j=1}^N w_{pop-1}^j K_{pop}(\theta_{pop-1}^{(i)}, \theta_t^{(i)})} & , \text{if } pop > 1 \end{cases}$$
8. If $i < N$, set $i = i + 1$ and returns to 3;
9. Normalize accepted particle weights;
10. If $pop < N_{pop}$, set $pop = pop + 1$ and returns to 2.

In the algorithm proposed by Toni et al. [50], it is necessary to define the total populations and the tolerances in each population. Then, for comparison between the simulated data and the experimental data, the Euclidean distance is used:

$$d(Y, Y^{meas}) = \sqrt{\sum_{i=1}^{N_t} (Y_i - Y_i^{meas})^2} \quad (15)$$

where N_t is the number of measurements.

The algorithm establishes that, while the particles are drawn from each population, the tolerances decrease monotonically. In the present work, the tolerances are sequentially adapted in each population using the average distances of the particles accepted in the previous population. Considering the samples of Euclidean distances obtained in a given last population, $(d_1^{pop-1}, d_2^{pop-1}, \dots, d_{N_{part}}^{pop-1})$, tolerance is calculated as follows:

$$\varepsilon_{pop} = \bar{d}^{pop-1} \quad (16)$$

While the algorithm proposed by Toni et al. [50] requires the imposition of the number of populations, in this work, Morozov's discrepancy principle was used as a stopping criterion [58]. We evaluated different transition kernels according to the following strategies:

1. Strategy 1: it was considered that the parameters of the models are not correlated.

Thus, the covariance between them is null. The parameters are drawn based on a Gaussian distribution, with the mean of the parameter value chosen randomly from the previous population.

$$\theta^* = N(\theta_{pop-1}^{l,m}; \sigma_{pop-1}) \tag{17}$$

- Strategy 2: it was considered that the parameters of the models are correlated. In this case, the covariance between them is different from zero. The parameters are drawn considering a normal multivariate Gaussian distribution, with the mean in the value of the parameter of the previous model, chosen through a resampling process, and standard deviation being the covariance matrix of all samples from the last population.

$$\theta^* = N(\theta_{pop-1}^{l,m}; \Sigma_{pop-1}^{cov}) \tag{18}$$

- Strategy 3: it was considered that the parameters of the models are correlated. Thus, the covariance between them was different from zero, and the parameters are drawn considering a Gaussian distribution, with multivariate normal, with the mean being the mean of all parameter values from the previous population and standard deviation being the covariance matrix of all samples from the last population.

$$\theta^* = N(\bar{\theta}_{pop-1}; \Sigma_{pop-1}^{cov}) \tag{19}$$

4. Results and discussion

The Approximate Bayesian Computational algorithm was used simultaneously to select models and estimate parameters using simulated measures. Besides, the verification of the algorithm was carried out through the four proposed models, using the three strategies.

In all numerical experiments, the measurements were obtained from model 4, considering uncertainties (σ_{meas}) equal to 1, 5, 10 and 30% of the maximum value of the size distribution density function, $n(D, t)$.

In the first strategy, the parameters of model 4, $\theta = [\beta_0 \ \sigma]$, are considered independent and not correlated; on the other hand, the second and third strategies admit that these parameters are correlated. 1000 particles were used in all estimates, and Morozov's discrepancy principle was adopted as the stopping criterion. The prior probability distribution of the parameters was adopted as uniform with support $U = [0\theta^m \ 4.0\theta^m]$ where m is the index for the model generating measure, which is model 4 in the present study. The parameters of the models are shown in Table 1.

Table 1. Reference values for the parameters of each model and prior probability distribution.

Parameter	Definition	Model Value	$\pi_{priori}(\theta)$
β_0	Constant		
	aggregation rate	1 e 4	1 cm ³ /s $U [0, 4]$
β_1	Linear		
	aggregation rate	2 e 3	1 cm ³ /s $U [0, 4]$
R_0	Removal rate	3	1 cm ³ /s $U [0, 4]$
σ	Growth rate	4	1 cm ³ /s $U [0, 4]$

Figure 2 shows the evaluation of tolerances at different levels of experimental uncertainty. The purpose of this analysis is to verify whether the tolerances were monotonically decreasing.

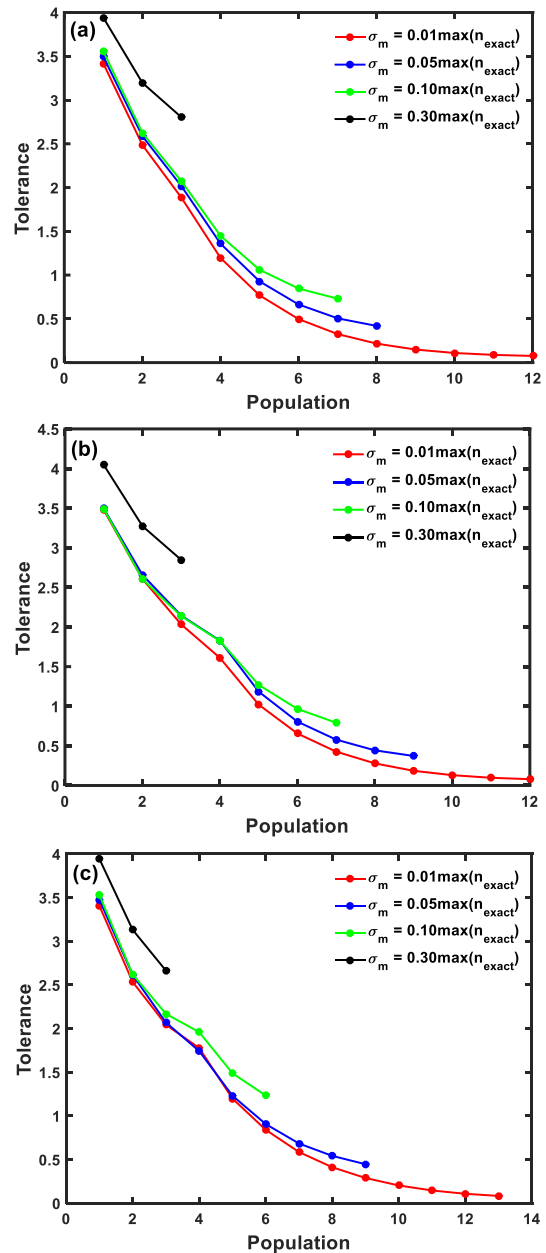


Figure 2. Evaluation of tolerance at different levels of experimental uncertainty for (a) strategy 1, (b) strategy 2 and (c) strategy 3

When analyzing Figure 2, it appears that the proposal to adjust the tolerances sequentially in each population satisfied the condition of being monotonically decreasing, as proposed by Tina Toni [59]. As there is an increase in the uncertainty of the measure, the number of populations needed to reach the stop criterion decreases. The results show that the stopping criterion was reached in the third population considering the experimental uncertainty of 30% of the maximum value of the size distribution density function, $0.30\max(n_{exact})$, for the three strategies adopted. While for the lowest level of experimental uncertainty assessed, $0.01\max(n_{exact})$, at least 12 populations were required.

After evaluating the proposed tolerance and stopping criteria, the estimates of parameters and state variables will be presented, considering the measures generated from model 4. Initially, it is analyzed whether the algorithm selected model 4 since this model originated the simulated measurements. Figure 3 shows the evolution of the model selection probabilities with the advance of the populations for the three transition kernel strategies analyzed.

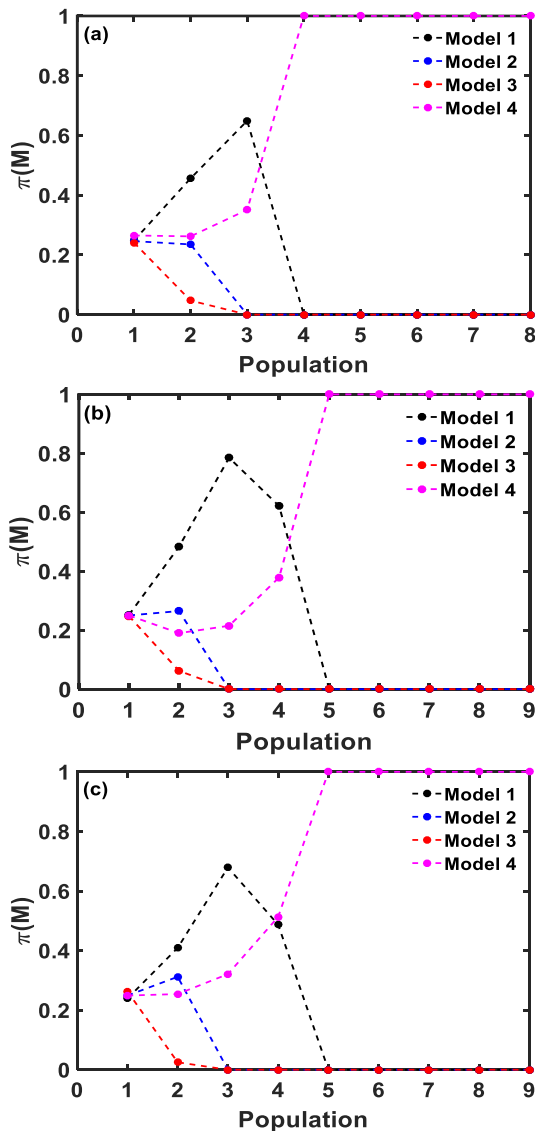


Figure 3. Probability of selecting the model in each population for (a) strategy 1, (b) strategy 2 and (c) strategy 3

Figure 3 shows that the algorithm correctly selected model 4 as the most suitable to represent the simulated measures. This selection is expected since model 4 generates the simulated measures. When evaluating the number of populations needed, it is observed that eight populations of the ABC algorithm were necessary to reach the stopping criterion. As seen in Figure 3, in the first population, all models are equiprobable. That is, they are equally likely to be selected. In population 3, models 2 and 3 have zero probability, so they are discarded from the selection algorithm. Only models 1 and 4 remain non-zero probability and stay in the competition to be selected. In population 3, model 1 has more considerable evidence than model 4, but from the fourth population, model 4 is selected. This behavior happens because the most significant evidence of model 1 concerning model 4 is related to Euclidean distances, $d(Y, Y^{meas})$ of each model accepted in the previous population. Information on Euclidean distances is presented in Table 2 - 4.

Table 2. Mean and standard deviation of Euclidean distances accepted for each model and in each population for strategy 1

Pop.	Tol.	Model 1	Model 2	Model 3	Model 4
1	3.49	2.55 ± 0.56	3.44 ± 0.42	4.62 ± 0.61	3.40 ± 1.17
2	2.59	2.39 ± 0.37	3.08 ± 0.20	3.21 ± 0.17	2.36 ± 0.79
3	2.02	2.21 ± 0.16	--	--	1.66 ± 0.59
4	1.36	--	--	--	1.36 ± 0.44
5	0.93	--	--	--	0.93 ± 0.27
6	0.66	--	--	--	0.66 ± 0.19
7	0.51	--	--	--	0.51 ± 0.09
8	0.42	--	--	--	0.42 ± 0.05

Table 3. Mean and standard deviation of Euclidean distances accepted for each model and in each population for strategy 2

Pop.	Tol.	Model 1	Model 2	Model 3	Model 4
1	3.49	2.57 ± 0.61	3.44 ± 0.44	4.61 ± 0.63	3.45 ± 1.23
2	2.66	2.40 ± 0.37	3.08 ± 0.22	3.22 ± 0.20	2.53 ± 0.74
3	2.14	2.24 ± 0.19	--	--	1.79 ± 0.63
4	1.83	2.07 ± 0.03	--	--	1.44 ± 0.46
5	1.18	--	--	--	1.18 ± 0.41
6	0.81	--	--	--	0.81 ± 0.24
7	0.58	--	--	--	0.58 ± 0.14
8	0.44	--	--	--	0.44 ± 0.08
9	0.37	--	--	--	0.37 ± 0.04

Table 4. Mean and standard deviation of Euclidean distances accepted for each model and in each population for strategy 3

Pop.	Tol.	Model 1	Model 2	Model 3	Model 4
1	3.48	2.56 ± 0.62	3.39 ± 0.45	4.65 ± 0.62	3.21 ± 1.27
2	2.61	2.30 ± 0.34	3.07 ± 0.21	3.24 ± 0.15	2.50 ± 0.73
3	2.07	2.16 ± 0.15	--	--	1.87 ± 0.54
4	1.74	2.03 ± 0.02	--	--	1.47 ± 0.44
5	1.23	--	--	--	1.23 ± 0.35
6	0.91	--	--	--	0.91 ± 0.23
7	0.68	--	--	--	0.68 ± 0.16
8	0.54	--	--	--	0.54 ± 0.09
9	0.45	--	--	--	0.45 ± 0.06

Tables 2-4 show the mean values of the Euclidean distances of the particles of each model in each population and their respective standard deviations. The tolerances, Tol, in each population are also shown. By analyzing the Tables, it's seen that for the three strategies used, the mean of Euclidean distances for model 1 is more significant than model 4 in population 3. In the same way, it's observed that these mean values are greater than tolerance. However, the standard deviations for model 1 are smaller than those for model 4. Thus, it is concluded that, although it presents greater evidence in the third population and, therefore, greater mean distances, few particles in model 1 are being accepted in that population. Thus, model 4, which is generating the measure, is selected starting from the fourth population.

After selecting the model, the correlation analysis was performed for the three transition kernel strategies evaluated. Correlation analysis is a tool to assess the possible two-way linear association between the aggregation coefficient, β_0 , and the growth rate, σ . Thus, this statistical evaluation also allows us to physically analyze how these parameters are associated. This analysis is contained in Figure 4.

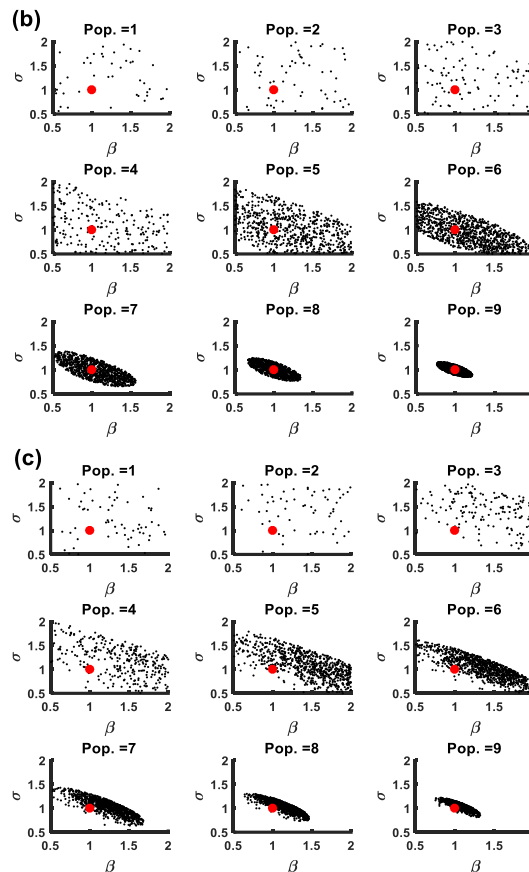
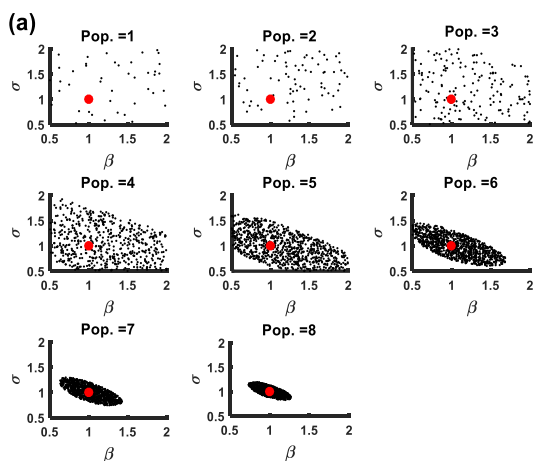


Figure 4. Correlation between the parameters of model 4 with advancing populations considering: (a) strategy 1, (b) strategy 2 and (c) strategy 3

In Figure 4, the red dot indicates the reference value of the parameters, while the black dots are samples of the posterior probability distribution in each population. In the first population, the points are dispersed because the parameters are initially considered uncorrelated and independent. That is, there is no linear relationship between them. As populations evolve, samples converge to values around the reference, indicating that uncertainties decrease and estimates show precision and accuracy. As populations advance, the correlation between parameters becomes more evident, as does the linear relationship between them. In the last population, the correlation has a negative slope. Evaluating this last population makes it possible to infer that the parameters are inversely related. As the value of one parameter increases the value of the other tends to decrease.

The correlation analysis between the parameters can help provide the physical behavior between the two evaluated parameters. The inverse relationship between them is expected since aggregation is a slower process and, consequently, usually occurs after the formation of molecules. In this way, the growth process is fast enough to form molecules of non-uniform size. With the inverse relationship between them, it is possible to infer that in physical-chemical processes in which agglomeration is the predominant phenomenon,

the growth rate will not influence the population density of particles of crystals, aerosols or polymers. Likewise, agglomeration may not affect dynamics when the growth rate is predominant.

It is important to emphasize that, although model 4 was selected in the 4th population, as shown in Figure 3 and Tables 2-4, the algorithm satisfied the stopping criterion only in the 8th population. This is because in the fourth population the estimates have not yet met the Morozov criterion, requiring more populations.

Tables 5 - 7 show the parameter estimates for the three transition kernel strategies evaluated for each model, considering only the last population. It appears that the estimated parameters of models 1, 2, and 3 showed values that were far from the exact value. However, both the parameters of models 2 and 3 have the exact and estimated values within the 99% credibility range. For the parameter β_0 from model 1, the estimated value showed a margin of 164% concerning strategy 1, 145% for strategy 2, and 143% for strategy 3. On the other hand, model 2 parameter, β_1 , have a deviation of 84% from the estimated regarding the exact value for strategy 1, 79% for strategy 2, and 90% for strategy 3. In addition, β_1 and R_0 , model 3 parameters, presented deviation of 13% and 38 % of exact values for strategy 1, 30% and 53% for strategy 2 and 54% and 57% for strategy 3, respectively.

As for the parameters of model 4, Tables 5-7 show that the estimates reached were precise (the parameters are within the 99% credibility range) and accurate (the parameters are close to the exact value). Estimated values of β_0 and σ showed deviations of 0.05% and 0.07%, respectively, for strategy 1, 2% and 1% for strategy 2, and 9% and 3% for strategy 3. Thus, the low values of deviation from the exact corroborate the accuracy of the estimates for the 3 strategies.

The estimation of the parameters of the population balance model is essential since, being a small-scale phenomenon, it is not possible to take direct measurements of the parameters. Furthermore, to define some parameters, such as the agglomeration coefficient, it is necessary to perform specific experiments. In addition to being expensive, these experiments have a high level of uncertainty.

Table 5. Estimation of parameters for strategy 1.

θ	Exact	Model 1	Model 2	Model 3	Model 4
β_0	$1 \text{ cm}^3/\text{s}$ (1.42; 4.06)	2.64	-	-	1.005 (0.74; 1.26)
β_1	$1 \text{ cm}^3/\text{s}$ -	1.84 (0.79; 2.74)	1.13 (0.03; 2.42)	-	-
R_0	$1 \text{ cm}^3/\text{s}$ -	-	0.62 (0.0003; 1.29)	-	-
σ	$1 \text{ cm}^3/\text{s}$ -	-	-	1.007 (0.84; 1.19)	-

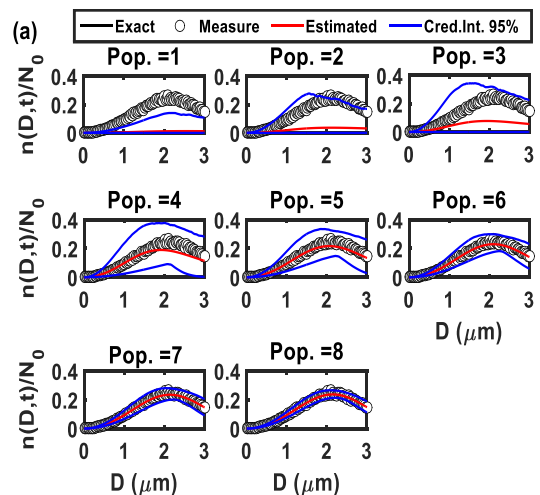
Table 6. Estimation of parameters for strategy 2.

θ	Exact	Model 1	Model 2	Model 3	Model 4
β_0	$1 \text{ cm}^3/\text{s}$ (1.90; 2.98)	2.45	-	-	0.98 (0.77; 1.21)
β_1	$1 \text{ cm}^3/\text{s}$ -	-	1.79 (0.76; 2.74)	1.30 (0; 3.08)	-
R_0	$1 \text{ cm}^3/\text{s}$ -	-	-	0.47 (0; 1.31)	-
σ	$1 \text{ cm}^3/\text{s}$ -	-	-	-	1.01 (0.85; 1.16)

Table 7. Estimation of parameters for strategy 3.

θ	Exact	Model 1	Model 2	Model 3	Model 4
β_0	$1 \text{ cm}^3/\text{s}$ (2.03; 2.81)	2.43	-	-	1.09 (0.80; 1.31)
β_1	$1 \text{ cm}^3/\text{s}$ -	-	1.90 (0.78; 2.70)	1.54 (0; 2.82)	-
R_0	$1 \text{ cm}^3/\text{s}$ -	-	-	0.43 (0; 1.13)	-
σ	$1 \text{ cm}^3/\text{s}$ -	-	-	-	1.03 (0.83; 1.21)

Figure 5 shows the size distribution density function for model 4 in each population for the three transition kernel strategies evaluated in terms of the measures and estimated values. The results presented correspond to the measurement in all particle diameters considering a time of 2 seconds. As expected, model 4 has a better agreement between the simulated and estimated measures since it generates the measures. It is also noted that, at the beginning of the process, the size density function increases due to the appearance of small molecules, but with the collision phenomena and consequent growth, the size density function decreases a lot. This phenomenon is explained by the fact that smaller molecules collide to form larger bodies, and thus the body in question grows, thus reducing the initial density.



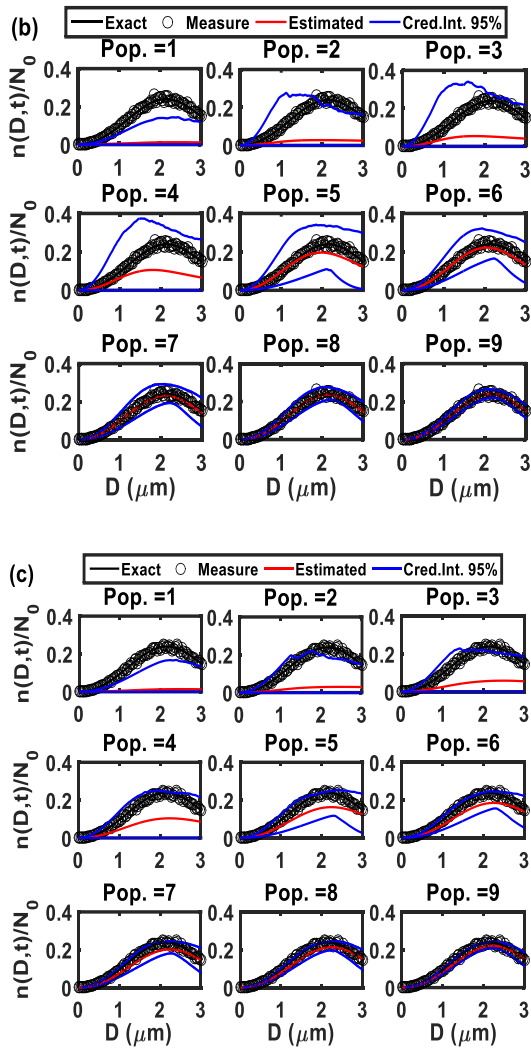


Figure 5. Estimates of the size distribution density function over time of 2 s for model 4 in terms of (a) strategy 1, (b) strategy 2 and (c) strategy 3

Figure 6 presents the correlation coefficient analysis for the three transition kernel strategies applied in the present work. Measurement uncertainty of 5% of the maximum value of the size distribution density function was considered. The evaluation of the correlation coefficients allows the analysis of the linear dependency relationship between the parameters of model 4.

For the measurement deviation analyzed for the three strategies, it is observed that in the first population, the correlation coefficient is equal to zero, indicating no correlation between the model parameters. As populations progress, the correlation coefficient decreases as the uncertainties in the estimates decrease, and the linear relationship between the parameters becomes more evident. Finally, the correlation coefficient stabilizes at negative values for all strategies, indicating a negative relationship between the two parameters. In other words, they are related in opposite directions - for a positive increase in, there is a decrease in and vice

versa. As stated before, this analysis allows us to assess how much the predominance of a physical phenomenon influences the occurrence of another.

For the 5% measurement deviation, comparing the results in Table 8 and Figure 11, the correlation coefficient for strategy 1 stabilizes around -0.65, showing a moderate correlation between the parameters [60]. For strategy 2, stabilization occurs at -0.7, while for strategy 3, it occurs at -0.85, indicating that for both, there is a strong negative correlation between the parameters [60].

Figure 7 presents how many times the straightforward model is solved in each population for the three strategies. The number of model solutions in each population is a critical analysis to assess the computational efficiency of the algorithm and the strategy implemented. Strategy 3 has the lowest computational cost among those analyzed, as it was the one that needed to solve the straightforward model less often.

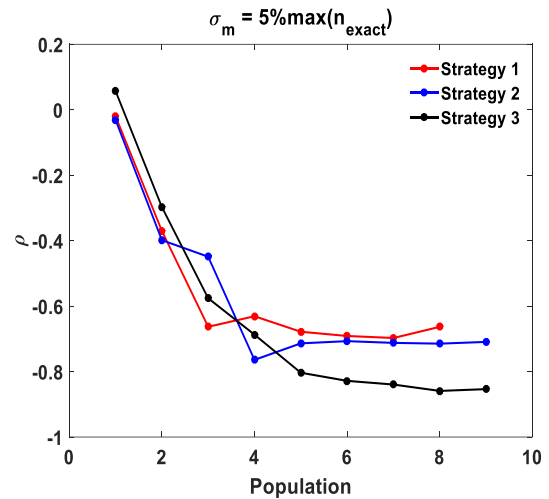


Figure 6. Correlation coefficients for the three strategies with an uncertainty of 5% in the measure

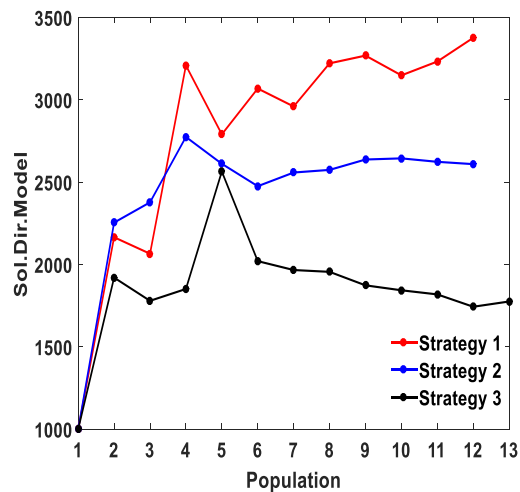


Figure 7. Straightforward model solutions using the three strategies implemented

Conclusion

In this work, the Approximate Bayesian Computation technique was applied to select models and estimate parameters simultaneously. In all cases studied, we observed that the proposed stopping criterion based on Morozov's discrepancy principle was adequate in determining tolerances in each population, as it met the criterion of monotonic reduction of tolerances with advancing populations.

Three different transition kernel strategies showed precise and accurate parameter estimates, demonstrating the good applicability of the technique and the importance of evaluating the influence of the correlation between the parameters in the transition kernel of the algorithm. Furthermore, the transition kernel of strategy 3 was the one that solved fewer times the direct model, being, therefore, the strategy that presents greater computational efficiency.

Thus, the Approximate Bayesian Computation technique proved to simultaneously select the models and estimate the parameters of the population balance equations studied in this work. The estimates of β_0 and σ have great physical significance as they represent physical mechanisms that govern population dynamics and are of fundamental importance in understanding the particle size distribution for any physical phenomenon that involves it. Besides, the algorithm can be a skillful method of application in a scenario in which different candidate models, which represent other hypotheses about population dynamics, are available, estimating the parameters of each model and selecting the one that best fits the experimental data available.

Nomenclature

D	Particle diameter [μm]
D_0	Initial particle diameter [μm]
$I_v(v,t)$	Rate of change of volume by mass transfer between particles and fluid phase [$\text{cm}^3.\text{s}^{-1}$]
K_t	Perturbation kernel
$meas$	Measures
$n(v,t)$	Size distribution density function [$\mu\text{m}^{-3}.\text{cm}^{-3}$]
$n(D,t)$	Size distribution density function as a function of diameter [$\mu\text{m}^{-1}.\text{cm}^{-1}$]
N_0	Total number of particles at time zero [cm^{-3}]
pop	Population
R_0	Removal Rate [$\text{cm}^3.\text{s}^{-1}$]
S_v	Net rate of addition or removal of particles in the system [$\text{cm}^3.\text{s}^{-1}$]
v	Particle volume [cm^3]
w	Importance weights
Y	Measurements Vector

Greek Letters

β_0	Constant aggregation coefficient [$\text{cm}^3.\text{s}^{-1}$]
β_1	Linear aggregation coefficient [$\text{cm}^3.\text{s}^{-1}$]
ε	Tolerance
L	Relationship between particle growth rate and aggregation rate
m	Mean
\mathbf{q}	Parameter Vector
Q	Relationship between particle removal rate and aggregation rate
$\pi(\boldsymbol{\theta} \mathbf{Y}^{meas})$	Posterior probability distribution
$\pi_{priori}(\boldsymbol{\theta})$	Prior probability distribution
$\pi(\mathbf{Y}^{meas} \boldsymbol{\theta})$	Likelihood function
r	Correlation coefficient
s	Growth rate [$\text{cm}^3.\text{s}^{-1}$]
S_{meas}	Measurements deviation
s_p	Standard deviation
t	Dimensionless time

Acknowledgements

The authors thank the CNPq, CAPES, FINEP, and PROPESP/UFPA for their financial support.

References

- [1] Naimi, L. J., Sokhansanj, S., Womac, A. R., Bi, X., Lim, C. J., Igathinathane, C., Lau, A. K., Sowlati, T., Melin, S., Emami, M. and Afzal, M., 2011. Development of a Population Balance Model to Simulate Fractionation of Ground Switchgrass. *Transactions of the ASABE*, 54(1), pp.219-227.
- [2] Hosseini, S. and Shah, N., 2011. Modelling enzymatic hydrolysis of cellulose part I: Population balance modelling of hydrolysis by endoglucanase. *Biomass and Bioenergy*, 35(9), pp.3841-3848.
- [3] Santos, T.C.S.S., Almeida, A.C.M., Pinheiro, D.R., Costa, C.M.L., Estumano, D.C., Ribeiro, N.F.P., Synthesis and Characterization of Colourful Aluminates Based on Nickel and Zinc, *Journal of Alloys and Compounds*, 2020, 815,152477. Sajjadi, B., Raman, A., Ibrahim, S. and Shah, R., 2012. Review on gas-liquid mixing analysis in multiscale stirred vessel using CFD. *Reviews in Chemical Engineering*, 28(2-3).
- [4] Singh, M. and Ramkrishna, D., 2013. A Comprehensive Approach to Predicting Crystal Morphology Distributions with Population Balances. *Crystal Growth & Design*, 13(4), pp.1397-1411.
- [5] Flood, A. and Wantha, L., 2013. Population balance modeling of the solution mediated transformation of polymorphs: Limitations and future trends. *Journal of Crystal Growth*, 373, pp.7-12.
- [6] Fernandes, R., Carlquist, M., Lundin, L., Heins, A., Dutta, A., Sørensen, S., Jensen, A., Nopens, I., Lantz,

- A. and Gernaey, K., 2012. Cell mass and cell cycle dynamics of an asynchronous budding yeast population: Experimental observations, flow cytometry data analysis, and multi-scale modeling. *Biotechnology and Bioengineering*, 110(3), pp.812-826.
- [7] Ramkrishna, D., 2000. *Population Balances*. Burlington: Elsevier.
- [8] Pinar, Z., Dutta, A., Bény, G. and Öziş, T., 2014. Analytical solution of population balance equation involving aggregation and breakage in terms of auxiliary equation method. *Pramana*, 84(1), pp.9-21.
- [9] Dutta, A., Pinar, Z., Constales, D. and Öziş, T., 2018. Population Balances Involving Aggregation and Breakage Through Homotopy Approaches. *International Journal of Chemical Reactor Engineering*, 16(6).
- [10] Randolph, A. and Larson, M., 1988. *Theory of particulate processes*. New York: Academic Press.
- [11] Cryer, S., 1999. Modeling agglomeration processes in fluid-bed granulation. *AIChE Journal*, 45(10), pp.2069-2078.
- [12] Rigopoulos, S. and Jones, A., 2003. Finite-element scheme for solution of the dynamic population balance equation. *AIChE Journal*, 49(5), pp.1127-1139.
- [13] Hede, P.D., 2006. *Modelling Batch Systems Using Population Balances*. Bookboon, London, UK.
- [14] Kumar, J., Peglow, M., Warnecke, G. and Heinrich, S., 2008. An efficient numerical technique for solving population balance equation involving aggregation, breakage, growth and nucleation. *Powder Technology*, 182(1), pp.81-104.
- [15] Shiea, M., Buffo, A., Vanni, M. and Marchisio, D., 2020. Numerical Methods for the Solution of Population Balance Equations Coupled with Computational Fluid Dynamics. *Annual Review of Chemical and Biomolecular Engineering*, 11(1), pp.339-366.
- [16] Rigopoulos, S., 2010. Population balance modelling of polydispersed particles in reactive flows. *Progress in Energy and Combustion Science*, 36(4), pp.412-443.
- [17] Marchisio, D. and Fox, R., 2005. Solution of population balance equations using the direct quadrature method of moments. *Journal of Aerosol Science*, 36(1), pp.43-73.
- [18] Kiparissides, C., Krallis, A., Meimaroglou, D., Pladis, P. and Baltas, A., 2010. From Molecular to Plant-Scale Modeling of Polymerization Processes: A Digital High-Pressure Low-Density Polyethylene Production Paradigm. *Chemical Engineering & Technology*, 33(11), pp.1754-1766.
- [19] Omar, H. and Rohani, S., 2017. Crystal Population Balance Formulation and Solution Methods: A Review. *Crystal Growth & Design*, 17(7), pp.4028-4041.
- [20] Naveira-Cotta, C., Cotta, R. and Orlande, H., 2010. Inverse analysis of forced convection in micro-channels with slip flow via integral transforms and Bayesian inference. *International Journal of Thermal Sciences*, 49(6), pp.879-888.
- [21] Naveira-Cotta, C., Cotta, R. and Orlande, H., 2011. Inverse analysis with integral transformed temperature fields: Identification of thermophysical properties in heterogeneous media. *International Journal of Heat and Mass Transfer*, 54(7-8), pp.1506-1519.
- [22] Moreira, P., van Genuchten, M., Orlande, H. and Cotta, R., 2016. Bayesian estimation of the hydraulic and solute transport properties of a small-scale unsaturated soil column. *Journal of Hydrology and Hydromechanics*, 64(1), pp.30-44.
- [23] Costa, J. and Naveira-Cotta, C., 2019. Estimation of kinetic coefficients in micro-reactors for biodiesel synthesis: Bayesian inference with reduced mass transfer model. *Chemical Engineering Research and Design*, 141, pp.550-565.
- [24] Knupp, D., Naveira-Cotta, C., Ayres, J., Orlande, H. and Cotta, R., 2012. Space-variable thermophysical properties identification in nanocomposites via integral transforms, Bayesian inference and infrared thermography. *Inverse Problems in Science and Engineering*, 20(5), pp.609-637.
- [25] Brock, J., Derjaguin, B., Drake, R., Hidy, G. and Yalamov, Y., 1971. *Topics in current aerosol research*. Oxford, New York: Pergamon Press.
- [26] Ramabhadran, T., Peterson, T. and Seinfeld, J., 1976. Dynamics of aerosol coagulation and condensation. *AIChE Journal*, 22(5), pp.840-851.
- [27] Gelbard, F. and Seinfeld, J., 1978. Numerical solution of the dynamic equation for particulate systems. *Journal of Computational Physics*, 28(3), pp.357-375.
- [28] Peterson, T., Gelbard, F. and Seinfeld, J., 1978. Dynamics of source-reinforced, coagulating, and condensing aerosols. *Journal of Colloid and Interface Science*, 63(3), pp.426-445.
- [29] Smoluchowski, M.V., 1916. Drei Vorträge über Diffusion, Brownsche Bewegung und Koagulation von Kolloidteilchen. *Zeitschrift für Physik*, 17, pp. 557-585.
- [30] Ilievski, D., 2001. Development and application of a constant supersaturation, semi-batch crystalliser for investigating gibbsite agglomeration. *Journal of Crystal Growth*, 233(4), pp.846-862.
- [31] Bekker, A. and Livk, I., 2011. Agglomeration Process Modeling Based on a PDE Approximation of the Safronov Agglomeration Equation. *Industrial & Engineering Chemistry Research*, 50(6), pp.3464-3474.
- [32] Barrasso, D., El Hagrasy, A., Litster, J. and Ramachandran, R., 2015. Multi-dimensional population balance model development and validation for a twin screw granulation process. *Powder Technology*, 270, pp.612-621.
- [33] Chaudhury, A., Tamrakar, A., Schöngut, M., Smrčka, D., Štěpánek, F. and Ramachandran, R., 2015. Multidimensional Population Balance Model Development and Validation of a Reactive Detergent Granulation Process. *Industrial & Engineering Chemistry Research*, 54(3), pp.842-857.
- [34] Kapur, P. and Fuerstenau, D., 1969. Coalescence Model for Granulation. *Industrial &*

- Engineering Chemistry Process Design and Development*, 8(1), pp.56-62.
- [35] Scott, W., 1968. Analytic Studies of Cloud Droplet Coalescence I. *Journal of the Atmospheric Sciences*, 25(1), pp.54-65.
- [36] Salman, A., Hounslow, M. and Seville, J., 2006. *Granulation, Volume 11*. Burlington: Elsevier.
- [37] Golovin, A. M., 1963. The Solution of the Coagulation Equation for Raindrops. Taking Condensation into Account. *Soviet Physics Doklady*, 8, pp. 191-193.
- [38] Hidy, G. and Brock, J., 1970. *International review in aerosol physics and chemistry*. Oxford; New York; Toronto: Pergamon Press.
- [39] Slama, M., Shaker, M., Aly, R. and Sirwah, M., 2014. Applications of aerosol model in the reactor containment. *Journal of Radiation Research and Applied Sciences*, 7(4), pp.499-505.
- [40] Tarantola, A., 2014. *Inverse Problem Theory*. Amsterdam: Elsevier Science.
- [41] Orlande, H., Colaço, M. and Dulikravich, G., 2008. Approximation of the likelihood function in the Bayesian technique for the solution of inverse problems. *Inverse Problems in Science and Engineering*, 16(6), pp.677-692.
- [42] Estumano, D.C., Hamilton, F.C., Colaço, M.J., Leiroz, A.J., Orlande, H.R., Carvalho, R.N., & Dulikravich, G.S., 2014. Bayesian estimate of mass fraction of burned fuel in internal combustion engines using pressure measurements. *Engineering Optimization IV - Proceedings of the 4th International Conference on Engineering Optimization*, pp. 997-1004
- [43] Pasqualetto, M., Estumano, D., Hamilton, F., Colaço, M., Leiroz, A., Orlande, H., Carvalho, R. and Dulikravich, G., 2016. Bayesian estimate of pre-mixed and diffusive rate of heat release phases in marine diesel engines. *Journal of the Brazilian Society of Mechanical Sciences and Engineering*, 39(5), pp.1835-1844.
- [44] Moura, C.H.R., Viegas, B.M., Tavares, M.R.M., Macêdo, E.N., Estumano D.C., Quaresma J.N.N., 2021. Parameter estimation in population balance through Bayesian technique Markov Chain Monte Carlo. *J. Appl. Comput. Mech.*, 7(2), pp. 890- 901.
- [45] Nunes, K., Dávila, I., Amador, I., Estumano, D. and Féris, L., 2021. Evaluation of zinc adsorption through batch and continuous scale applying Bayesian technique for estimate parameters and select model. *Journal of Environmental Science and Health, Part A*, 56(11), pp.1228-1242.
- [46] Oliveira, R., Nunes, K., Jurado, I., Amador, I., Estumano, D. and Féris, L., 2020. Cr (VI) adsorption in batch and continuous scale: A mathematical and experimental approach for operational parameters prediction. *Environmental Technology & Innovation*, 20, p.101092.
- [47] Pritchard, J., Seielstad, M., Perez-Lezaun, A. and Feldman, M., 1999. Population growth of human Y chromosomes: a study of Y chromosome microsatellites. *Molecular Biology and Evolution*, 16(12), pp.1791-1798.
- [48] Marjoram, P., Molitor, J., Plagnol, V. and Tavaré, S., 2003. Markov chain Monte Carlo without likelihoods. *Proceedings of the National Academy of Sciences*, 100(26), pp.15324-15328.
- [49] Sisson, S., Fan, Y. and Tanaka, M., 2007. Sequential Monte Carlo without likelihoods. *Proceedings of the National Academy of Sciences*, 104(6), pp.1760-1765.
- [50] Toni, T., Welch, D., Strelkowa, N., Ipsen, A. and Stumpf, M., 2008. Approximate Bayesian computation scheme for parameter inference and model selection in dynamical systems. *Journal of The Royal Society Interface*, 6(31), pp.187-202.
- [51] Beaumont, M., Cornuet, J., Marin, J. and Robert, C., 2009. Adaptive approximate Bayesian computation. *Biometrika*, 96(4), pp.983-990.
- [52] Tavaré, S., Balding, D., Griffiths, R. and Donnelly, P., 1997. Inferring Coalescence Times From DNA Sequence Data. *Genetics*, 145(2), pp.505-518.
- [53] Beaumont, M., Zhang, W. and Balding, D., 2002. Approximate Bayesian Computation in Population Genetics. *Genetics*, 162(4), pp.2025-2035.
- [54] Lenormand, M., Jabot, F. and Deffuant, G., 2013. Adaptive approximate Bayesian computation for complex models. *Computational Statistics*, 28(6), pp.2777-2796.
- [55] Amador, I.C.B., Nunes, K.G.P., De Franco, M.A.E, Viegas, B.M., Macêdo, E.N., Féris, L.A., Estumano, D.C., 2022. Application of Approximate Bayesian Computational Technique to Characterize the Breakthrough of Paracetamol Adsorption in Fixed Bed Column. *International Communication in Heat and Mass Transfer* 132, pp.105917.
- [56] Toni, T. and Stumpf, M., 2009. Simulation-based model selection for dynamical systems in systems and population biology. *Bioinformatics*, 26(1), pp.104-110.
- [57] Toni, T., Stumpf, M., 2009. Tutorial on ABC rejection and ABC SMC for parameter estimation and model selection.
- [58] Morozov, V.A., 1966. On the solution of functional equations by the method of regularization. *Soviet Mathematics Doklady*, 7, pp. 414-417
- [59] Toni, T., 2010. *Approximate Bayesian computation for parameter inference and model selection in systems biology*. Imperial College London (University of London).
- [60] Mukaka, M.M., 2012. Statistics corner: A guide to appropriate use of correlation coefficient in medical research. *Malawi Medical Journal*, 24, pp. 69-71.
- [61] Ilievski, D. and White, E., 1994. Agglomeration during precipitation: agglomeration mechanism identification for Al(OH)₃ crystals in stirred caustic aluminate solutions. *Chemical Engineering Science*, 49(19), pp.3227-3239.